# Supporting Information

## Hybrid AuNP@GCD nanosensor for dual mode dopamine detection and imaging in drosophila brain

Lingaraj Behera,[a] Lopamudra Mishra,[b] Monalisa Mishra,[b,c] Sasmita Mohapatra [a,c]*

*[a] Department of Chemistry, National Institute of Technology, Rourkela, India-769008, E-mail: sasmitam@nitrkl.ac.in

[b] Department of Life Science, National Institute of Technology, Rourkela, Odisha 769008, India

[c] Centre for Nanomaterials, National Institute of Technology, Rourkela, Odisha 769008, India

**Contents in the supporting information:**

**Figure S1** TEM of GCD

**Figure S2** XRD analysis of GCD and AuNP@GCD

**Figure S3** Hydrodynamic size of GCD and AuNP@GCD

**Figure S4** TEM image of (a) Au NP (b-d) AuNP@GCD nanoprobe at various magnification(e) AFM image of AuNP@GCD(f) Topographic height of AuNP@GCD

**Figure S5** EDAX and elemental mapping of AuNP@GCD

**Figure S6** FTIR of GCD

**Figure S7** (a) Survey, (b)C 1s, (c) O 1s, (d) N 1s (e) B1s (f) Au 4f of XPS spectra

**Figure S8** (a) UV -absorbance spectra of GCD and AuNP@GCD (b) excitation dependent emission spectra of GCD (c) FL emission intensity of GCD after conjugation of EDEA(d)FL intensity of GCD after AuNP addition

**Figure S9** FL stability of (a) AuNP(b)AuNP@GCD

**Figure S10** (a) pH of the AuNP@GCD, pH of AuNP@GCD after the addition of dopamine (b) FL with increasing conc. of the probe (c) Time dependent PL emission after and before addition of dopamine

**Figure S11**(a) Absorbance and emission study of AuNP and GCD (b) Fluorescence life time study (c) HD size of GCD after AuNP addition (d) HD size of GCD@AuNP after DA addition

**Figure S12** The DPV responses of 0.1 M DA in 0.1 M PBS

**Figure S13** selectivity study

**Figure S14** The DPV curves after immediate washing for three times showing the reusability of the sensor; (B) The peak currents of five independently coated electrodes showing the reproducibility of AuNP@GCD/GCE (C) DPV profiles obtained for 0.1M DA on AuNP@GCD/GCE showing the stability of the sensor for 20day

**Figure 15** DAPI and DCFH-DA staining (a-d) bright field image, (e-h) image of DCFH-DA treated gut after treatment of AuNP@GCD (i-l) DAPI treated gut (m-p) merged image (q) impact of AuNP@GCD on the micronucleus

**Figure 16** NBT Assay

**Figure 17** Eyes, thorax, wings adult phenotype image. In control (a, e, i) and treated concentrations of 100 µg/ml (b, f, j), 150 µg/ml (c, g, k), and 200 µg/ml (d, h, l).

**Figure 18** Trypan blue staining assay showing the effect of AuNP@GCD in the 3$^{rd}$ instar larval stage (a) No indication of cell disruption in control larvae (b) 100µg/ml, (c)150µg/ml, and (d)200µg/ml AuNP@GCD treated larvae did not indicate any internal gut damage

**Figure 19** The mean interaction plot of the larval crawling speed of (a) Control and (b, c, and d) 100, 150, and 200 µg/ml, respectively, in all treated groups.

**Figure 20** Climbing assay in each nanocomposite treated setup comparable with control flies; behavioural abnormality was not significantly found with increases up to 150 µg/ml concentration

**Figure 21** No Significant differences were observed in touch sensitive score of treated flies at 100,150 and 200 µg/ml as compared to control

**Figure 22** Light/dark preference assay of larva, Petri dishes. (a) Control and (b−d). 100, 150, and 200 µg/ml doses of the hybrid nanocomposite treated larval groups, respectively, (e) Graph of the light/dark preference test (N = 15 (60 larvae) per time point)

**Instrumentation**

A UV-VIS spectrophotometer (Shimadzu 2650) and a spectrofluorometer (PTI-Horiba QuantaMaster QM-400 fluorimeter) were utilised to measure UV-visible absorption and fluorescence spectra. Particle size and zeta potential data were measured by using a zeta sizer Nano ZS 90, Malvern instrument. Fourier Transform Infrared Spectroscopy (FTIR) (IRAffinity-1S, Shimadzu, spectrophotometer) was utilised to know the surface functional groups. The graphitic amorphous structure and phase content of the as prepared nanocomposite were obtained through X-ray diffraction technique by using a Rigaku Ultima-IV X-ray diffraction instrument equipped with Cu $K_\alpha$ radiation ($\lambda$ = 0.1542 nm). The XRD measurements were performed at a scan rate of 2$^o$/min in the 2$\theta$ range of 5$^o$ to 90$^o$ by using Bragg-Brentano configuration The energy dispersive X-ray spectroscopy (EDX) along with elemental mapping images were obtained using an Oxford EDS detector attached as an accessory to the FESEM instrument. The TEM study was checked by using a FEI Tecnai G2 TF30-ST instrument operating at an accelerating voltage of 300 kV. The surface composition of AuNP@GCD was

examined by X-ray photoelectron spectrum (XPS) recorded by (PHI 5000 VersaProbe III). A Bruker Multimode-8 atomic force microscope (AFM) was used to examine the surface topography and sample roughness. The average fluorescence lifetime was calculated by using a Horiba Jobin von TCSPC (time-correlated single-photon counting technique). Using a spectrophotometer with an integrating sphere and the software Felix GX 4.1.2, the absolute photoluminescent quantum yield is calculated. The fluorescence dopamine imaging in *Drosophila* brain cells was visualized through confocal microscope by using Leica instrument (Leica, TCS SP8).

**Synthesis of green carbon dot (GCD)**

Green carbon dots of size < 10 nm were synthesized from red cabbage (B. oleracea). The red juice extracted from the crushed red cabbage was heated for 8h at 180°C in an autoclave reactor lined with poly(tetrafluoroethylene). Subsequently, the solution was permitted to cool naturally. To separate the larger carbon particles with lower fluorescence, the brown solution underwent filtration. The filtrate underwent ultracentrifugation at 5,000 rpm for 15 min. The GCD solution underwent dialysis for 24 hours using deionized water and a 0.22 µm porous membrane filter. After dialysis, GCD solution was concentrated and collected after freeze-drying. The lyophilized GCD powder was dispersed in the aqueous solution of EDEA.

**Synthesis of Au nanoparticle**

Au NPs were synthesized by the reduction of $HAuCl_4$ using sodium citrate as a reducing agent. 240 mg of $HAuCl_4$ was mixed in 500 mL of distilled water and was stirred till mixing. Then the solution was heated to boiling with the addition of 50 mL of sodium citrate solution (1%) and the stirring was continued for the next 1 h. After 1 h, a wine-red solution was obtained with an absorption maximum at 520 nm.[1]

**Synthesis of 3-APBA modified AuNP**

The synthesis of AuNP was explained in the supporting information (SI). 3-APBA can attach to the surface of AuNPs via electrostatic interaction with the citrate ions on the AuNP surface, without causing a noticeable change in the ruby red color of the AuNPs. The colloidal solution of 3-APBA-assembled AuNPs is created by simply combining AuNPs (approximately 5 nM) with different concentrations of 3-APBA (0.5 to 1 M) in 1 mM PBS at pH 7.

**Preparation of electrolyte (0.1 M PBS)**

The 0.1 M PBS buffer solution with pH 7.4 was prepared by mixing of standard stock solutions of 0.1 M sodium dihydrogen phosphate monohydrate (M=137.99 g/mol, 3.45g in 250 mL) and 0.1 M disodium hydrogen phosphate dehydrate (M=178.00 g/mol, 4.45 g in 250 mL) in suitable amounts.[2]

**Dopamine detection in real sample**

Human serum of three different person were collected from a CWS Hospital, Rourkela. The human serum centrifuged at high speed (5000 rpm) for 5 min. The supernatant was collected, and different concentrations of dopamine were added to 3 mL of the supernatant to prepare a series of test samples. The FL detection of human serum samples was conducted under the same conditions, except that the dopamine standard was replaced by dopamine containing samples. The FL spectra of dopamine spiked systems were measured after incubation for 5 min. The content of dopamine in samples was calculated from the plotted linear relationship between dopamine and $F/F_0$.

**Fabrication of electrode of Electrochemical (EC) sensing**

Glassy carbon electrodes (GCE) were cleaned by using an alumina powder polishing kit. The GCE was subsequently cleaned using ultrasonic methods for 10 min in normal water. This cleaning process was repeated after every analysis. To make the modified electrodes, all samples (AuNP@GCD/GCE, GCD/GCE, AuNP/GCE and bare GCE) were gently placed on the cleaned surface of the GCE. Then, allowed to dry at room temperature (RT).

## Cytoxicity, genotoxicity, and phenotype study

The toxicity of the AuNP@GCD probe was evaluated in *Oregon R strain* of Drosophila melanogaster as per our recently published paper.[3] The cytotoxic effect of AuNP@GCD was studied on all phenotypes of drosophila. Twenty flies were examined for any abnormalities in their eyes, wings, and thorax. Adult phenotype images of all flies were taken using a stereo microscope.[4]

## Optimization of sensing parameters

The sensor performance can be significantly influenced by experimental parameters like pH value, probe concentration, and reaction time. The analysis was examined under the optimal experimental conditions. The change in FL intensity with respect to pH was examined. As mentioned in figure S10a, the FL intensity of GCD gradually increased with rising pH values, peaking at 7. Therefore, neutral condition (pH 7) was selected for this sensing system**.** To optimize the probe concentration in sensing experiments, 50 µM dopamine solution was mixed to various conc. of AuNP@GCD solutions (4, 2, 1, 0.5 µg/mL) at pH 7. The highest $F/F_0$ value is observed in the solution with an AuNP@GCD concentration of 2 µg/mL. At very low conc. of AuNP@GCD, the fluorescence on intensity ($F/F_0$) is less due to fewer active sites of the dopamine. At higher concentrations of nanoconjugate, the binding sites are less available, leading to non-specific interaction. A conc. of 2 µg/mL of AuNP@GCD was employed for all experimental analyses (Figure S10b). The FL intensity of AuNP@GCD was recorded after the drop wise addition of dopamine with respect to time. When 50 µM of dopamine solution was added to the AuNP@GCD solution, the FL intensity of the AuNP@GCD was increased up to 40 mins and reaches a plateau (Figure S10c)

## Physical behavioural study of *Drosophila* in presence of AuNP@GCD

## Experimental procedure

### Fly strain management and culture

The *Oregon R* strain of D. melanogaster has been as a model organism for in vivo glycine sensing. The flies were fed with a diet that included 4g of sucrose, 0.8g of type I agar, 5g of corn meal, and 2.5g of yeast. All these ingredients were moved to a glass bottle and 100 ml water was added. The food bottle and culture vials (sealed with cotton plugs) were kept in an autoclave bag. The food was autoclaved for 45 min and then, it was placed under laminar flow to cool. To prevent the risk of microbial and fungal contamination, propionic acid (300 mL) an antifungal agent and nipagine (500 mL) an antimicrobial agent was added to the diet. The flies are moved to new food vials in a ratio of 7 female: 5 male. They were kept at a temperature 25$^{o}$C with 60% humidity, and 12 h-light and dark cycle. A stock solution of AuNP@GCD in water (2 mg/ml) was made by mixing the nanocomposite with water, and stored at low temperature. Food was prepared for both control and treatment flies. After preparation, the AuNP@GCD was not given to the control flies. In contrast, in the case of the treatment flies, various concentrations of AuNP@GCD were fed. After a period of 4 days, the third instar larvae were developed and were subsequently utilized for further experiment.[5]

### Application in real sample

### Trypan blue study

From trypan blue image allows for the differentiation between live and dead cells. A positive trypan blue stain indicates that there is no damage to the gut after administering the AuNP@GCD nanocomposite in the food vial. Even at higher concentrations, the treatment of the AuNP@GCD nanocomposite did not result in any damage to the larval gut. (Figure S19) All the information suggests that our AuNP@GCD fluorescent probe is completely safe for use in bioimaging applications.

### Measurements of Oxidative Stress after AuNP@GCD Treatment on Larvae

Haemolymph collected from larvae in their 3$^{rd}$ instar was used to calculate oxidative stress. Briefly, 30 numbers of 3$^{rd}$ instar larvae were collected. The larvae were cooled in a box and pricked near the thorax to stop melanization. Centrifugation of larvae was performed at 4°C for 15 min at 5000 rpm (Eppendorf-centrifugation 5430/5430R, Germany). 10 µL of hemolymph was taken in an Eppendorf tube of 2 mL, and 10 µL of 1X phosphate-buffered saline (PBS) was added to the tube. An equal volume of 1.5 mM nitroblue tetrazolium (NBT) solution (11383213001, Sigma-Aldrich, Merck, Germany) was added to the mixture and left for 60min in the dark. NBT assay was performed on the hemolymph according to the protocols of Nayak et al. 2020 and Bag et al. 2020.[6,7] NBT (1.5 M) solution was given to the hemolymph and left for 60min in the dark. The reaction was stopped after 60min by adding an equivalent amount of 100% glacial acetic acid (GAA) (A6283, Sigma-Aldrich, Merck, Germany) and incubating for 10 min. Then, 150 µL of 50% GAA was mixed and 200 µL of the solution was

poured in the well of a 96-well plate, and the absorbance was taken at 595 nm with the help of a microplate reader (Elisa Biobase, EL10A).

**Living and non-living cell analysis**

To test the cytotoxicity in the gut cells of the larva, trypan-blue dye was applied. Six third-instar larvae sample were collected to check the toxicity of AuNP@GCD. The larvae were rinsed with 1X PBS to clean and separate the cuticular food remnants. They were stacked up into a 1 ml tube, and the tube was further wrapped using an aluminium foil. Trypan-blue (93595, Sigma-Aldrich) (0.2%) was pipetted to the tube and kept for 60 min under dark conditions. After 1 h of the incubation period, the larva was washed using 1X PBS for 2–3 times to remove excess stain. The larvae were checked one after one under the stereo zoom camera, and the presence of stain in the gut was observed.

**Larvae crawling behavior Assay**

The crawling assay was done with six third instar larva from each treatment concentration 100µg/ml,150µg/ml,200µg/ml of AuNP@GCD nanocomposite and control.[5] Larva from different treatment vials were collected and washed by using 1X PBS to remove the food particles. A crawling plate was made using 2% agar poured in a petri plate to provide a surface for larval crawling.[8]An agar plate was made for initial acclimatization of larvae to crawling surface. One by one, the larvae were picked to the centre of a different agar plate and a graph paper was placed beneath to trace the path. Meanwhile, the photo was taken (SAMSUNG M51). The time taken by each larvae to reach the periphery of the petri plate was measured, and that time was divided by 60sec to measure the crawling speed. On the agar gel, the larvae left a trailing impression/mark of their travelled path. A black marker was used to sketch the larvae's crawling routes, and their average speed per second was then plotted.

**Climbing Assay**

Climbing is an innate behavior of *Drosophila*. *Drosophila* always tries to climb vertically against gravity, so they showed negative geotactic behavior. Adult fruit flies locomotory behavior was evaluated using this same technique as in a reported protocol.[9] 7-days old flies (30 adult flies) were moved to the climbing apparatus from three distinct concentrations.[10,11] Flies were taped gently to the bottom of the vial, and the duration of 10 s to climb 16 cm of the tube was recorded. All concentrations of the nanocomposite and control were tested nine times using this methodology. Percentages of total flies were used to determine the number of flies in each group that successfully climbed the mark of 16 cm in the time of 10s.

**Touch sensitivity Study**

The central nervous system, different body segments and neuromuscular junctions works in a coordinated manner to produce a sensation i.e., referred to as touch. The brain of drosophila contain central pattern generators (CPG) is considered as the main source of this stimuli. The movement is possible due to oscillatory network even in the absence of the

external sensory input. However, without a feedback loop from the peripheral nervous system (PNS), the larva's body segments expansion and contraction occurs in an uncoordinated manner. In the late embryonic stage, the signals from the CPG initiates peristatic movement and it remains throughout the larval stage. The CPG signals the chordotonal organ of the PNS for locomotion as well as sensation.[12] Therefore, any sensory damage in the larvae will obstruct the larvae to respond to the stimuli. From this assay, larval behaviour is studied and the neuronal defect can be scored. The exact procedure is followed for isolating the larva, washing and acclimatization in the agar plate environment. For providing mechanical stimuli to larvae, toothpick was glued with a soft eyelash. This was used in gently pricking the thoracic segments of the larvae. The responses of the larvae were recorded and noted. This was scored according to Dhar et. Al. 2020.[13]

**Larval light/dark Preference Assay**

This experiment is used to detect an early photoreceptor deficiency using the approach described by Sabat et al. 2016.[14] A Petri dish was divided into four quadrants, with the opposite quadrant being colored black (two quadrants are black). Then, 1% agarose was added and let to set. Fifteen third instar larvae from both the control and treatment vials were kept in the dark for 6h before the experiment began. The larvae were placed on the agar plate, and the lid with the same marking as the Petri plate was closed. The Petri dish was illuminated uniformly, and the larvae were given 5 min to move freely between the dark and light sections. After 5 min, we removed the lid and images were captured. Each batch of larvae performed the test three times, and the experiment was conducted in five sets.[9,14]

**Result and Discussion**

**ROS Analysis**

An NBT (11383213001, Sigma-Aldrich, Merck, Germany) assay was performed in the third instar larval haemolymph to measure the amount of intracellular ROS. ROS formation increased significantly in the AuNP@GCD treated group as compared to the control. Thus, the NBT assay suggests that the ROS scavenging activity decreased with increase in AuNP@GCD nano-composite as shown in (Figure 13). In control, the absorbance value at 595 nm was found to be 0.151 ± 0.016. In 100 µg/ml concentration, the value increased to 0.166 ± 0.013. In 150 µg/ml concentration, the absorbance was further increased to 0.174 ± 0.012, and for 200 µg/ml concentration, the absorbance was 0.202 ± 0.009. The absorbance of the NBT assay is directly proportional to the quantity of ROS generated, which ultimately correlates with the level of oxidative damage to the cells. The amount of ROS formation that occurs compared to the control is represented in the graph (Figure 13).[6,15]

**Crawling Assay**

The crawling behavioral test is a more practical assay to explore the neuronal abnormalities in an early stage of larva for the neuronal mechanosensory investigation. The crawling behavior of third instar larvae was studied in the *Drosophila* model. The neuronal toxicity

caused by the nanocomposite exposure can disrupt the coordinated crawling of larvae. The healthy larvae move in a straight line, whereas the abnormal ones zigzag and sometimes slow down. Thus, the crawling assay is preferable for identifying abnormalities in gene expression that might result in fatalities during the pupal and adult stages. In the crawling assay, no distinct curve or turn has been recorded for the control larvae. There was no significant crawling path change for the treatment concentrations of 100 µg/ml and 150 µg/ml, whereas a significant change was seen in 200µg/ml concentration. In the control vial of larvae, 0.907 ± 0.034 were able to cover the distance in mm/s, whereas 0.855 ± 0.049 were able to cover the distance in 100 µg/ml, 0.834 ± 0.030 in 150 µg/ml and 0.591 ± 0.050 in 200 µg/ml. The crawling speed of third instar larva clearly indicate that the treatment of 100 µg/ml and 150µg/ml larvae significantly covers the same distance in mm/s comparable to control larva, whereas the crawling speed of 200µg/ml treated third instar larva was significantly reduced and shows more zig-zag and slow motion mainly indicating neuronal defects or changes. The larvae tracking paths and the crawling speed plot is demonstrated in Figure S14.

**Climbing Assay**

The climbing experiment describes the behavioral changes that occur in flies in response to gravity. The number of flies that could ascend to 16 cm in the 10 s is used to analyze this test. In due order, the number of flies that could climb up to 16 cm was normalized to 100%. The assay was performed 9 times (N = 9) for each concentration, including control. In the control flies vial, 94.44 ± 3.25 were able to climb, whereas 84.77 ± 11.99 in 100 µg/ml, 81.44 ± 15.77 in 150µg/ml, and 71.33 ± 21.30 in 200 µg/ml were able to climb up to the 16 cm mark. The result of the climbing assay is plotted in a graph shown in Figure S15. The climbing ability was seen nonsignificant up to 40µg/ml of treated flies compared to the control flies of the setup.

**Touch Sensitivity Test**

In our experiment, we found that there is no significant change in touch sensation in the treatment concentrations of 100µg/ml,150µg/ml,200µg/ml. For 100µg/ml nanocomposite treatment, the larva touch sensitivity score was 2.76 ± 0.33, which was practically identical to the control group score that was 2.91 ± 0.27 (the scores for both groups were more than 2 but below 4, indicating that larvae mostly retract and then move but sometimes turn $90^0$). Similarly, at 150µg/ml and 200µg/ml concentration the touch sensitivity score was 2.81 ± 0.26 and 2.68 ± 0.20 respectively (the scores for both groups were in between 2 and 3, indicating that the larvae hold their movement before moving forward) as shown in figure S16.

**Larval Light-Dark preference assay**

The larva's light preference test was done to look for any early defects in the light-sensing neurons. In this experiment, the percentage of larvae attracted to light decreased as the concentration of nanocomposite treatment increased. The control group's percentage of larvae attracted to light was 62.66 ± 7.60%. There were 41.33 ± 5.57% in 100 µg/ml, 35.99 ± 5.96% in 150 µg/ml, 33.33 ± 8.16% of light-sensitive larvae in 200µg/ml as shown in Figure

S17. However, light was avoided or dark was preferred by 37.33 ± 7.60% larvae from the control group, 58.66 ± 5.57% in 100µg/ml, 63.99 ± 5.96% in 150 µg/ml, 66.66 ± 8.16% in the case of 200 µg/ml AuNP@GCD nanocomposite-treated larval group

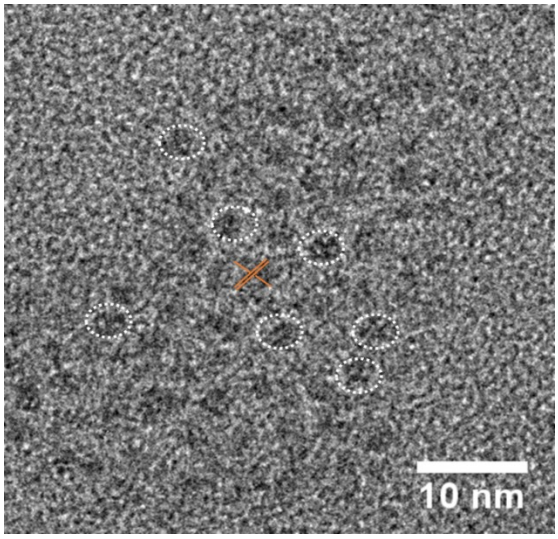


**Figure 1**

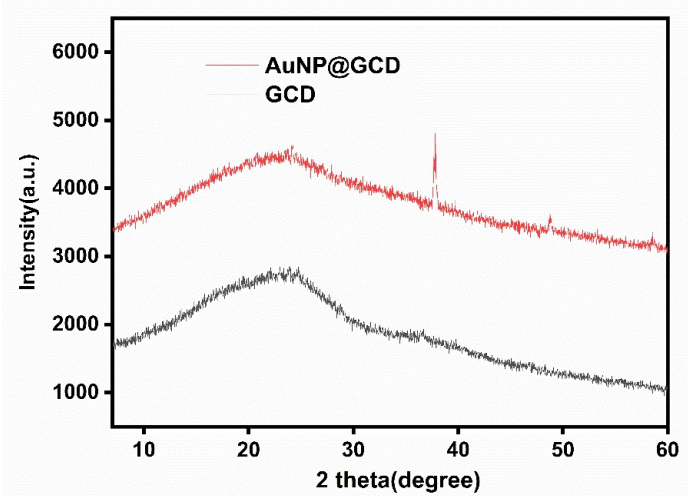


**Figure 2**

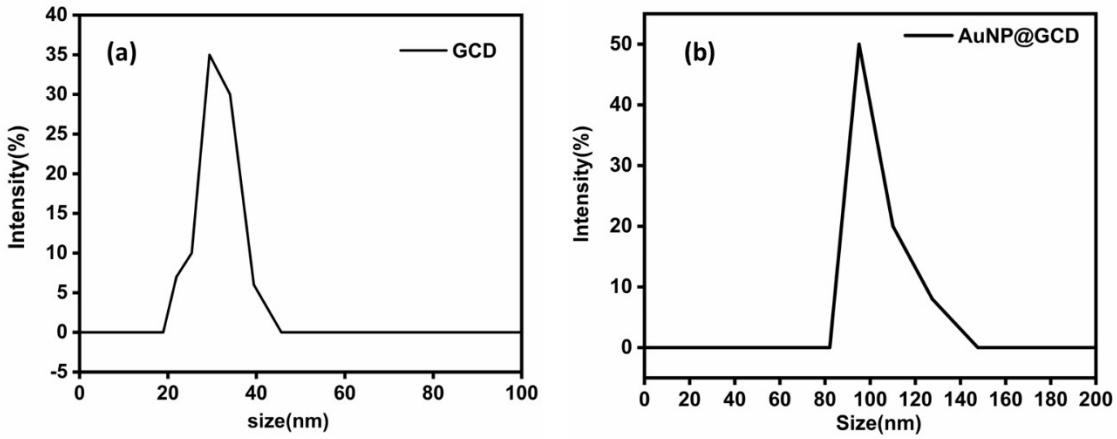


**Figure 3**

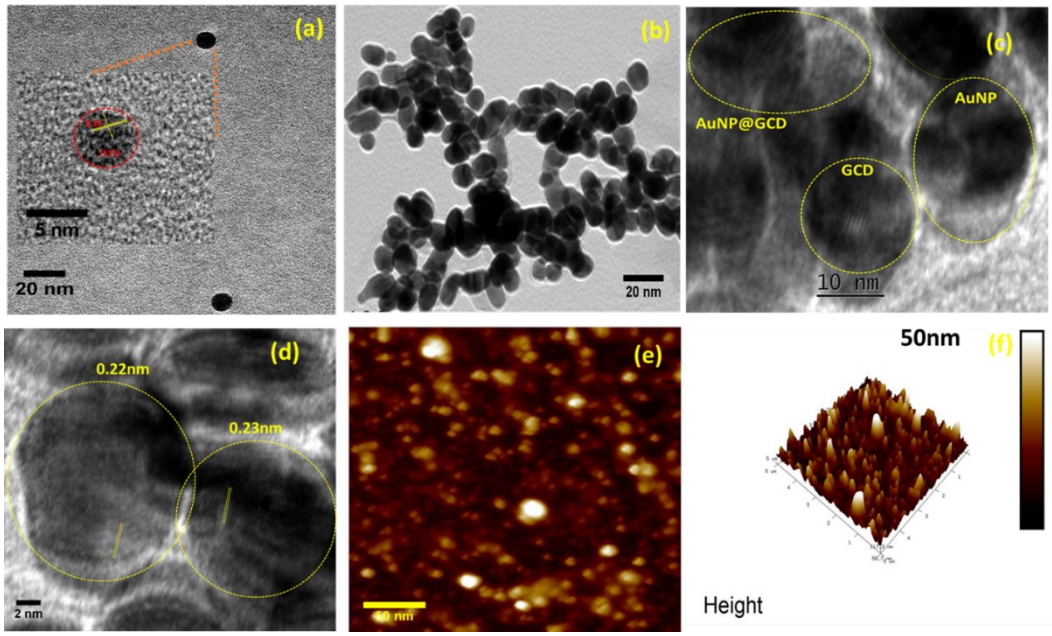


**Figure 4**

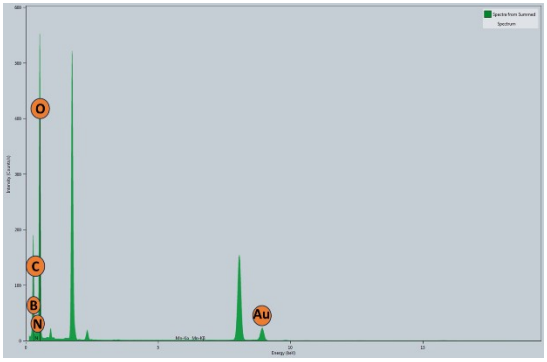


| Element | Weight% | Atomic% |
|---|---|---|
| C K | 35.70 | 30.23 |
| N K | 16.80 | 13.25 |
| O K | 44.95 | 40.50 |
| B K | 1.07 | 1.02 |
| Au L | 1.48 | 15 |
| Totals | 100 | |

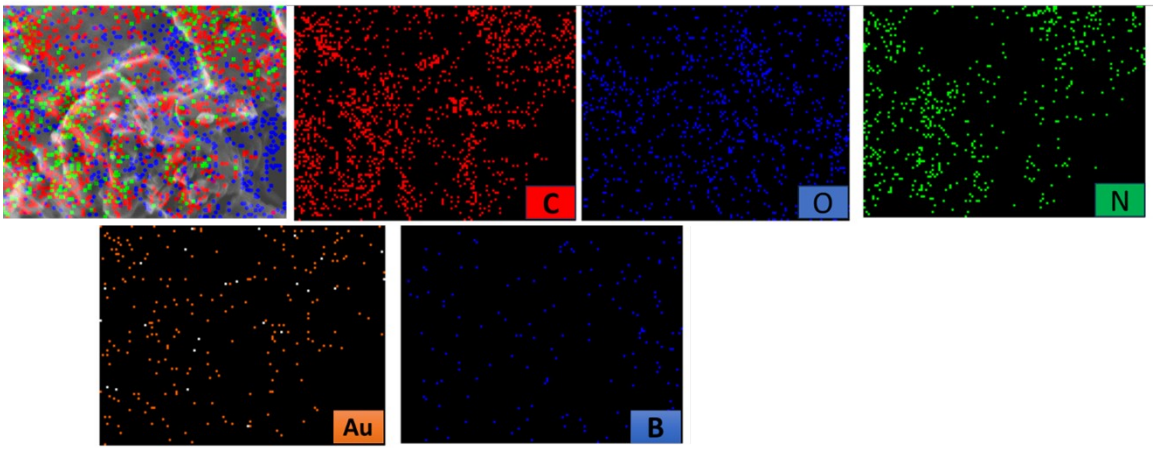


**Figure 5**

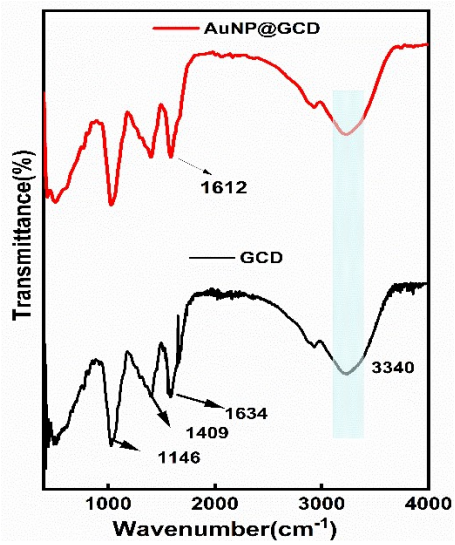


**Figure 6**

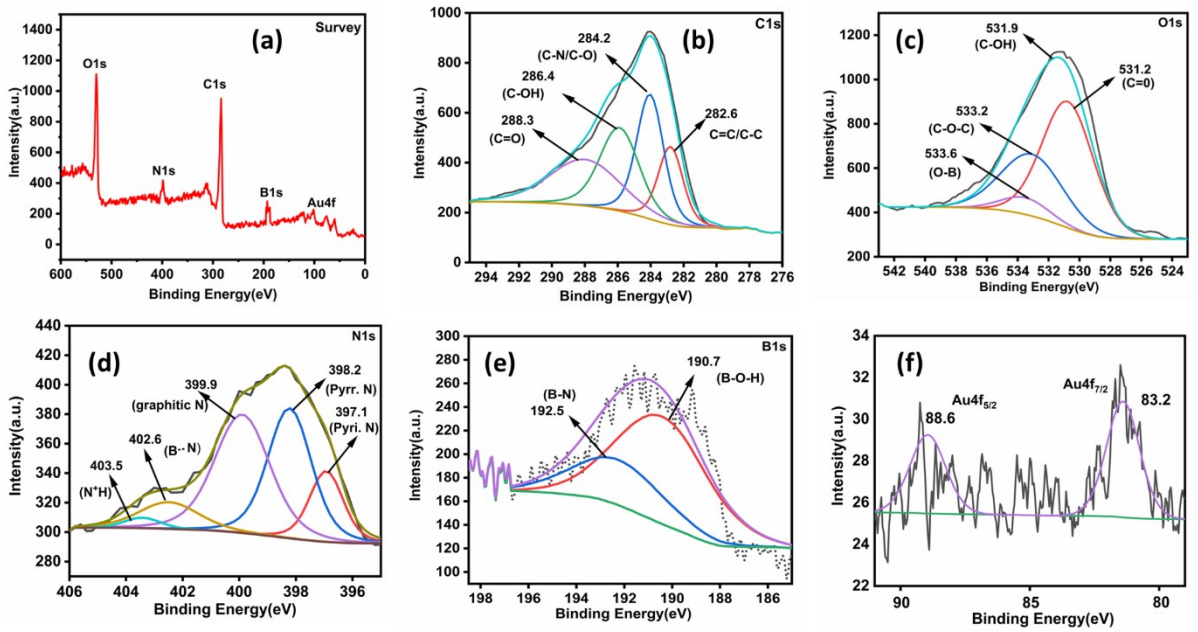


**Figure 7**

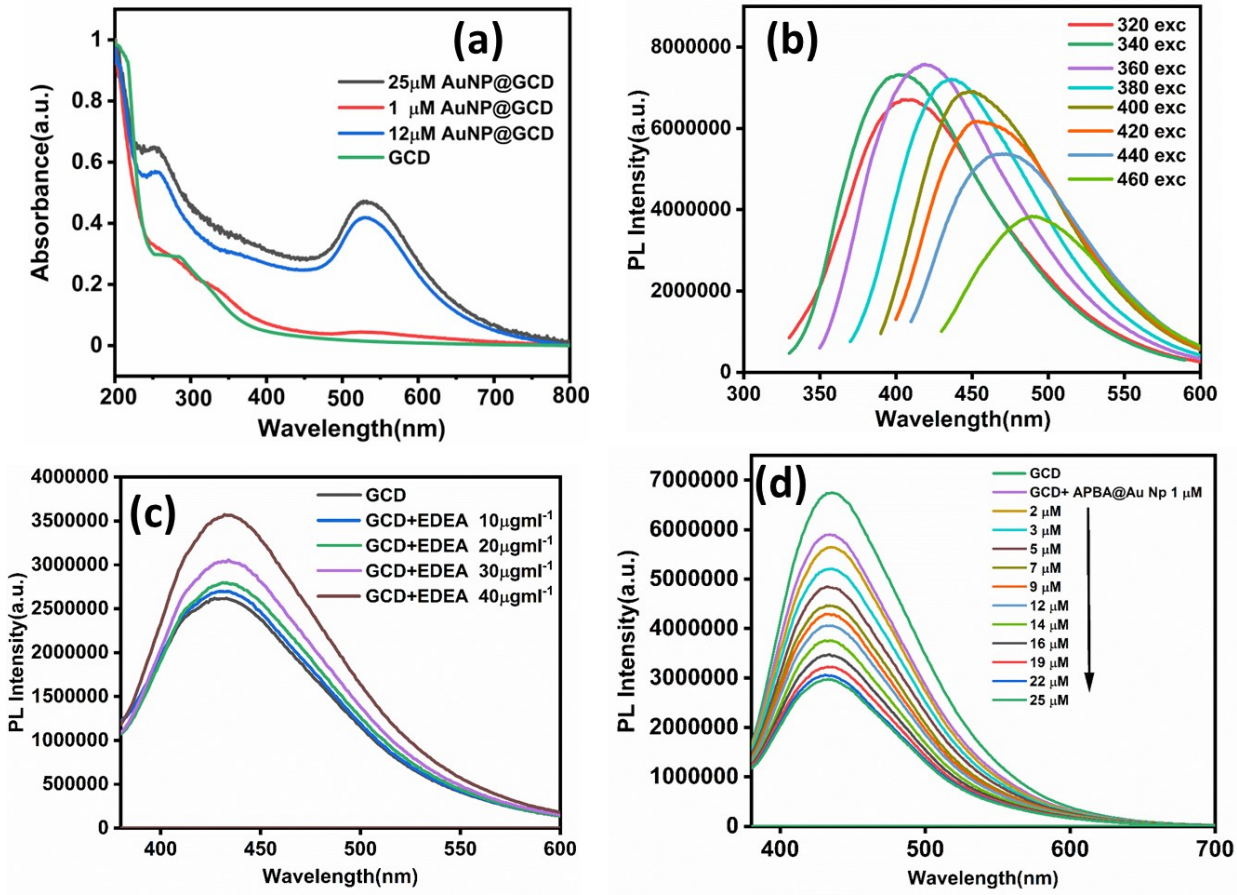


**Figure 8**

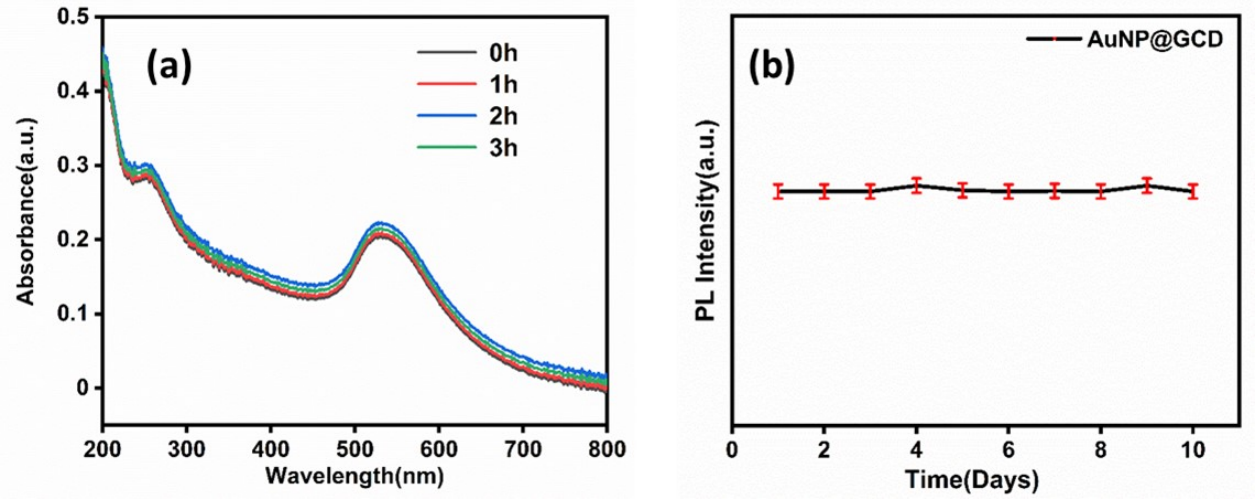


**Figure 9**

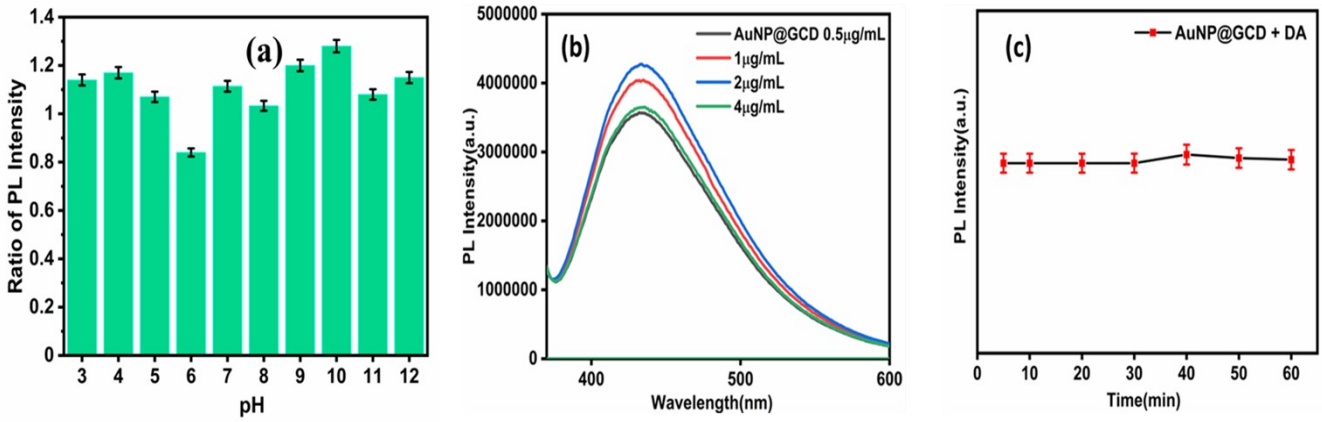


**Figure 10**

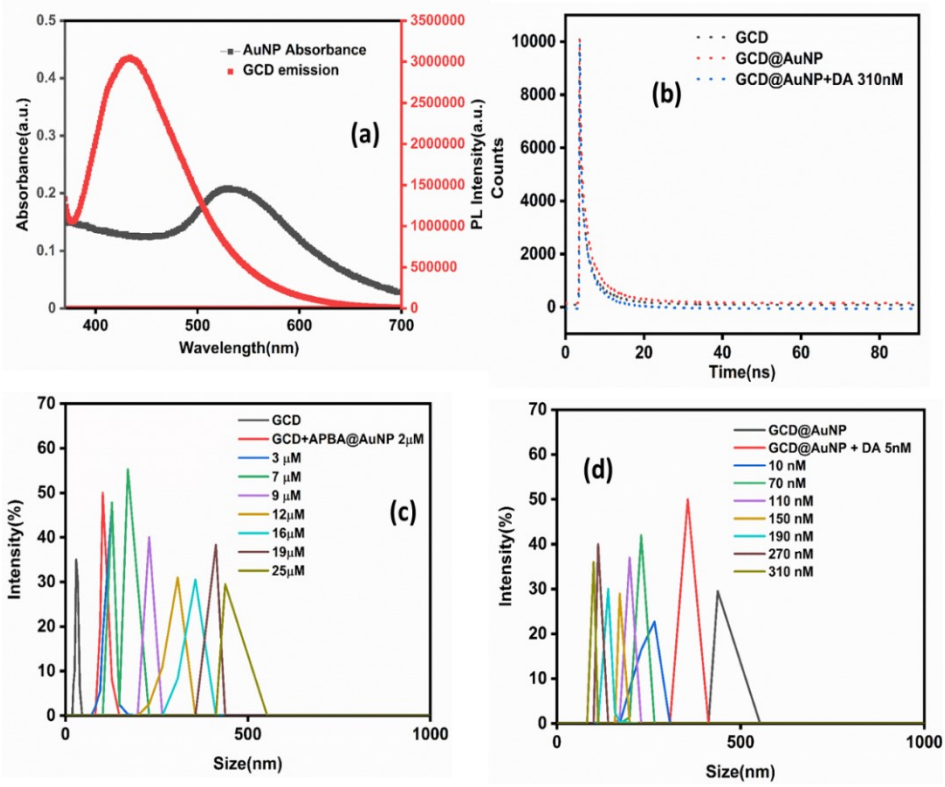


**Figure 11**

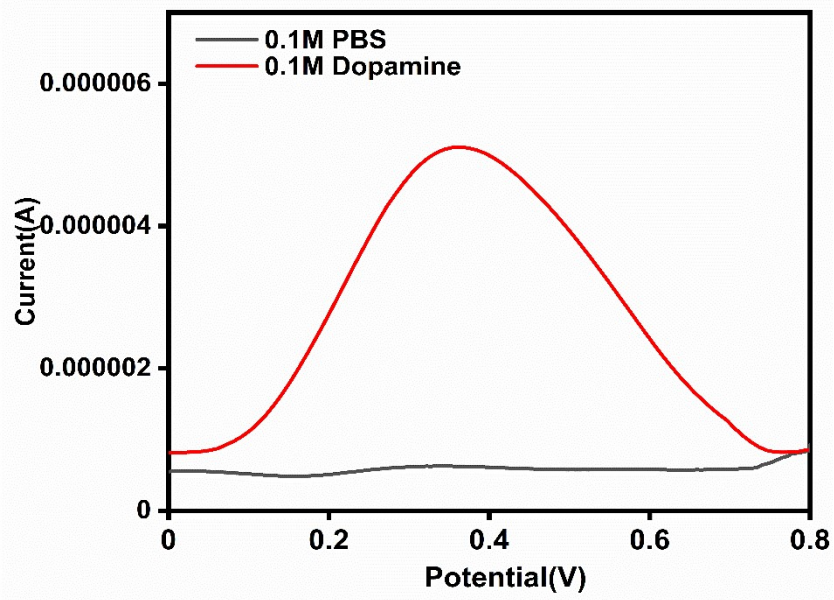


**Figure 12**

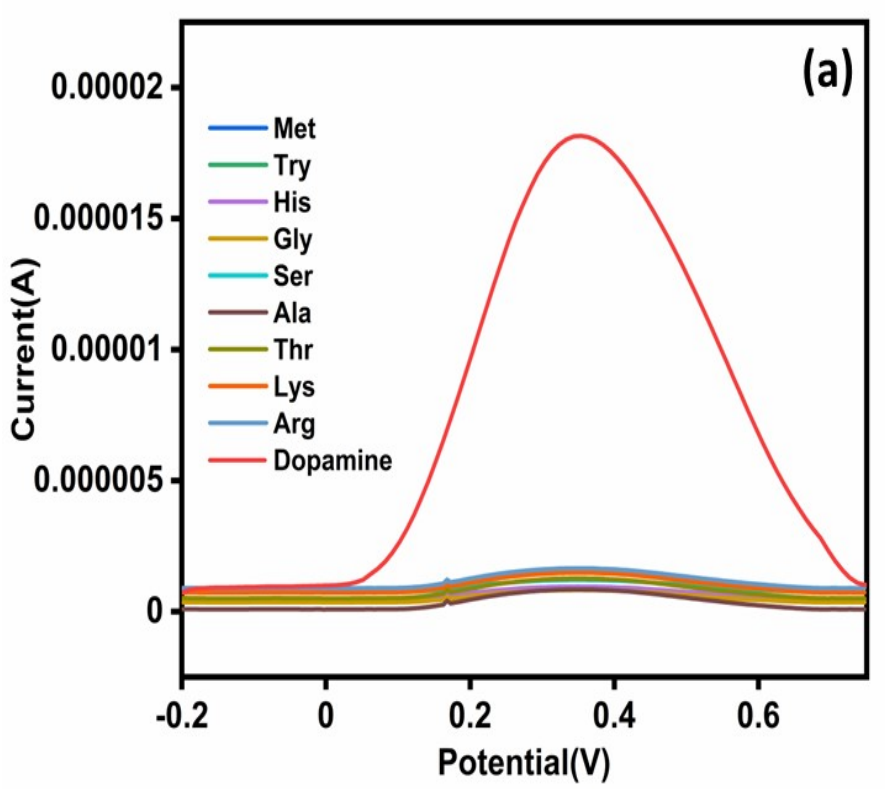


**Figure 13**

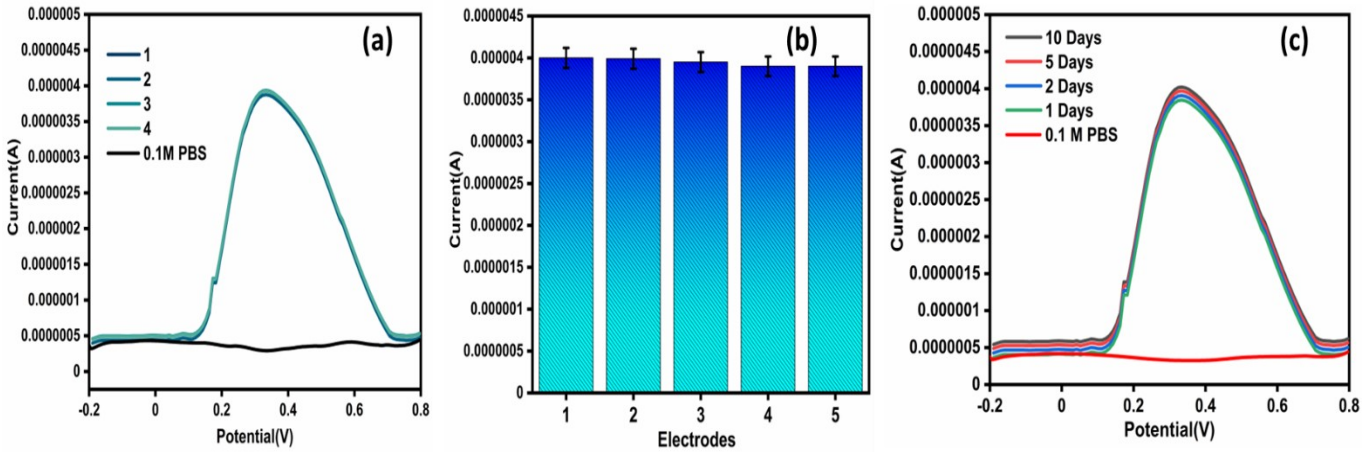


**Figure 14**

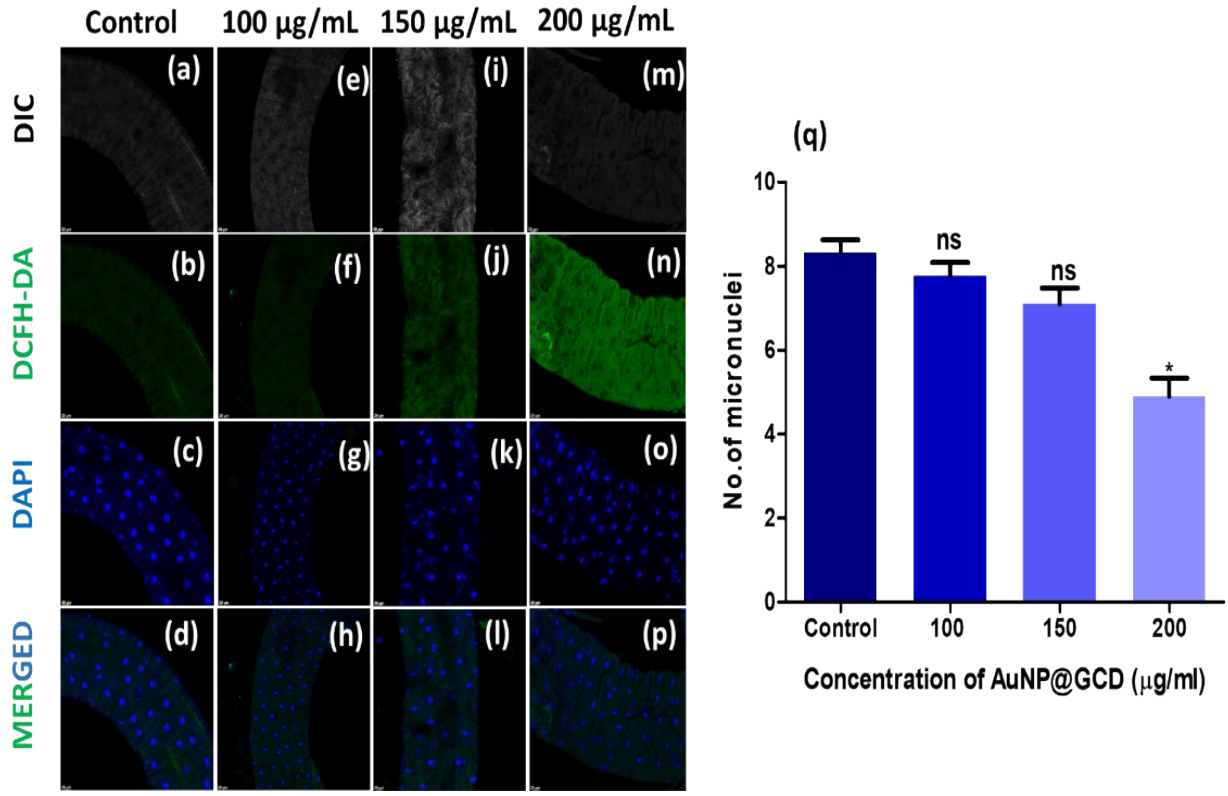


**Figure 15**

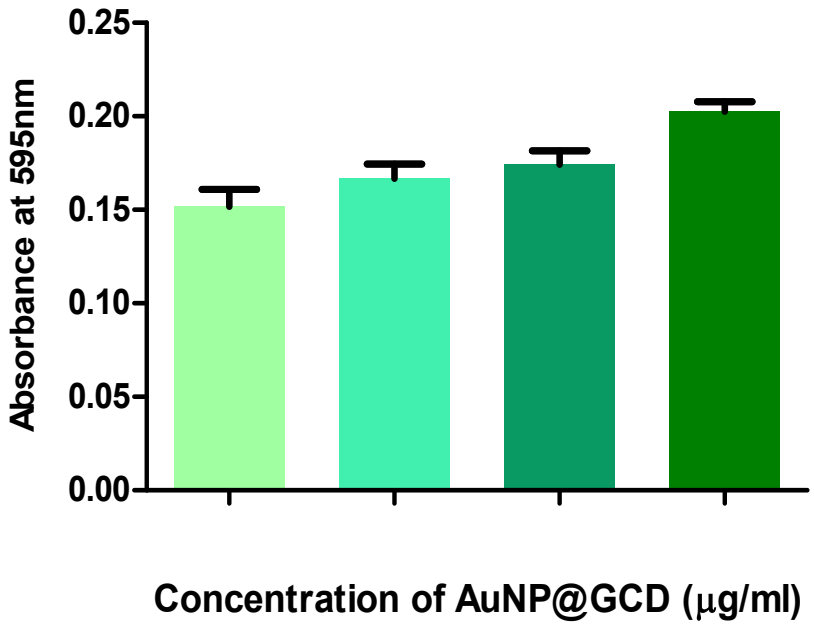


**Figure 16**

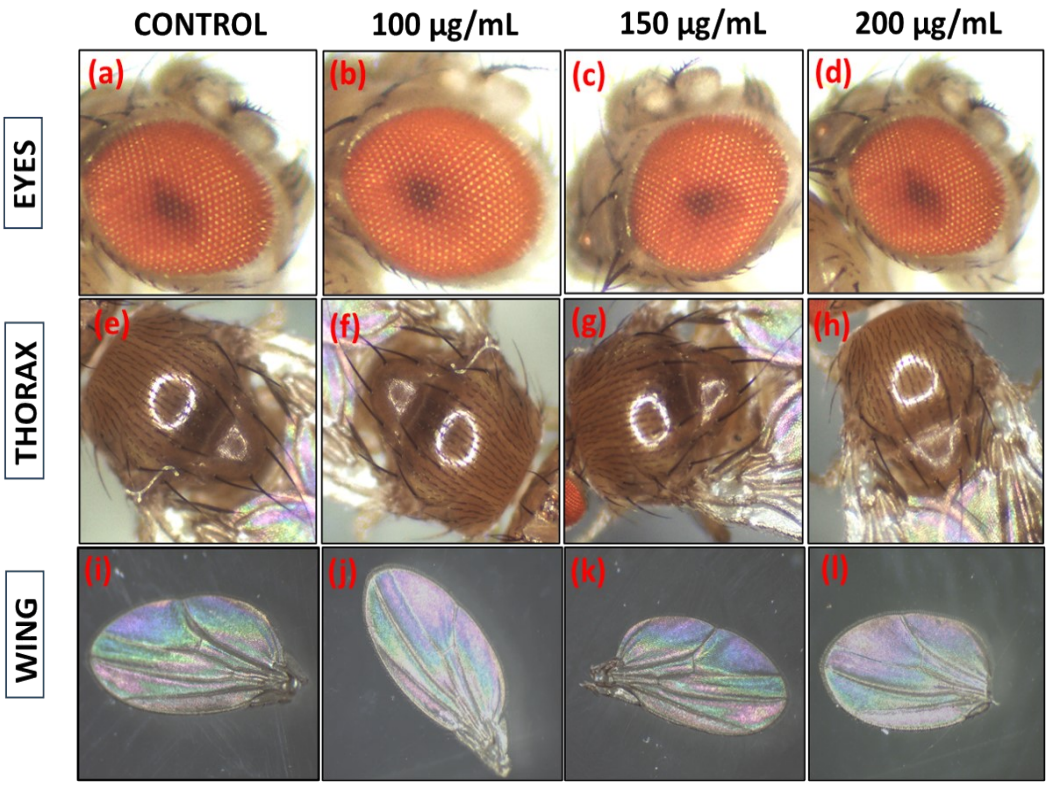


**Figure 17**

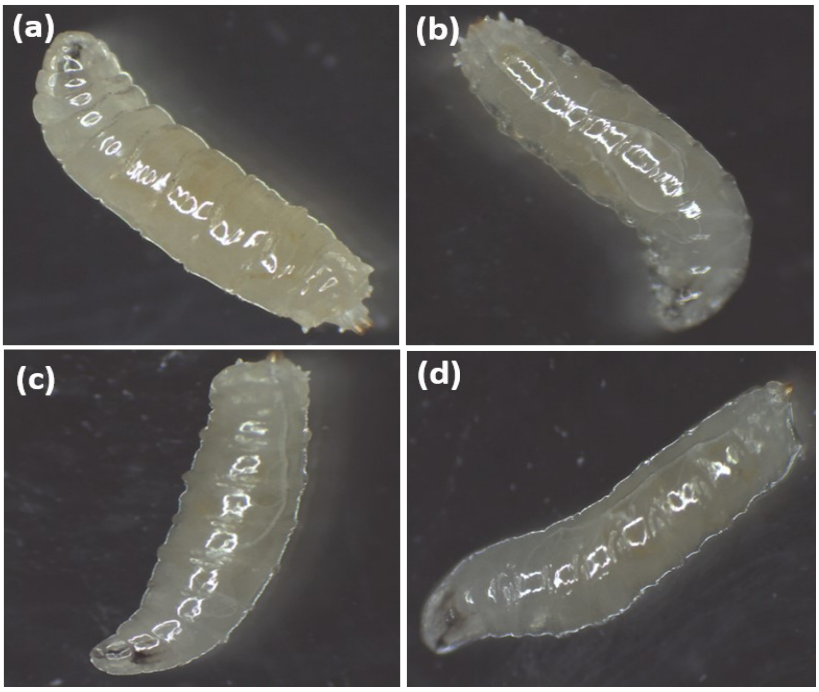


**Figure 18**

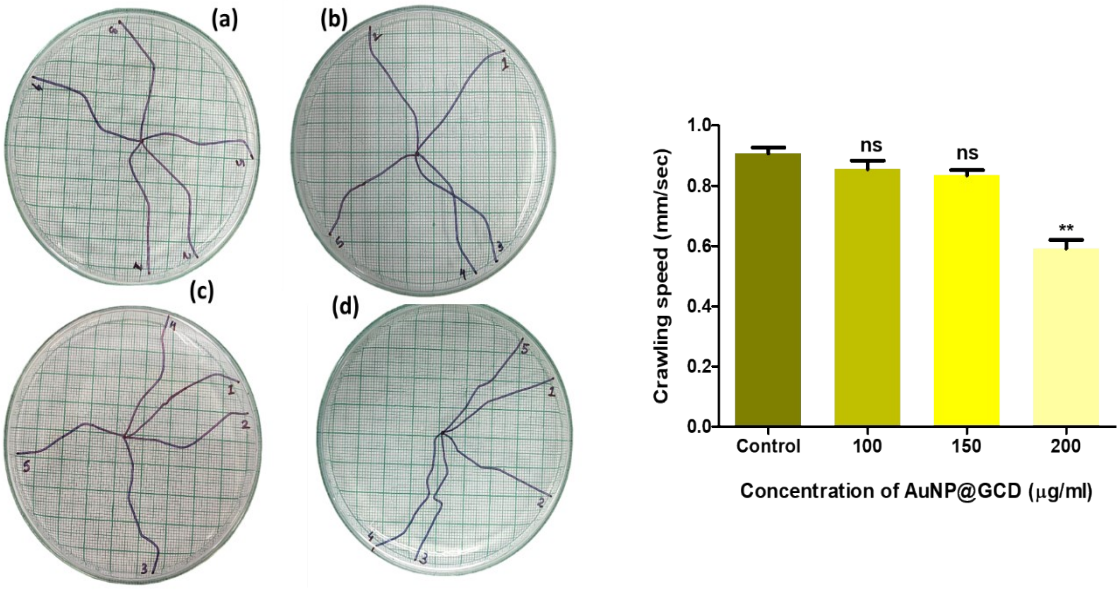


**Figure 19**

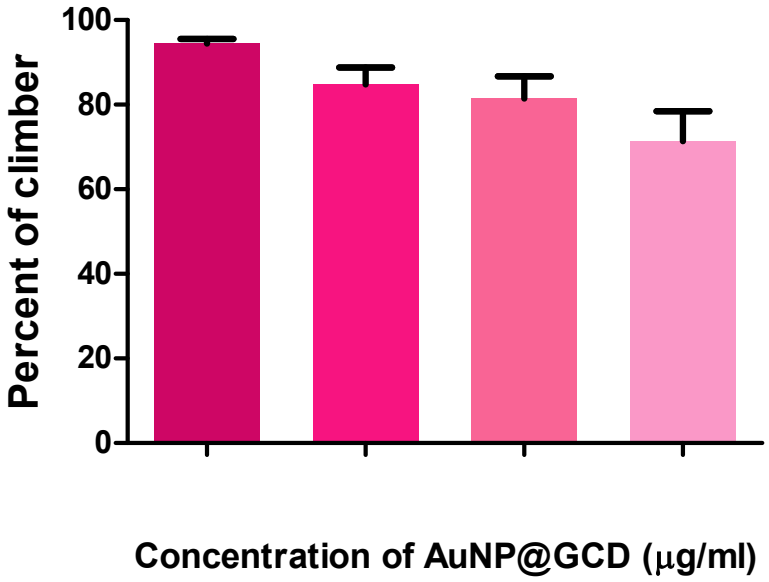


**Figure 20**

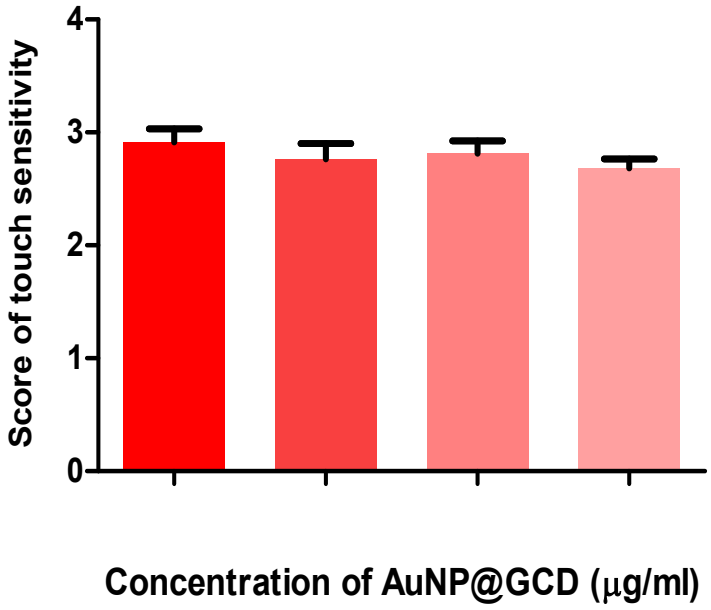


**Figure 21**

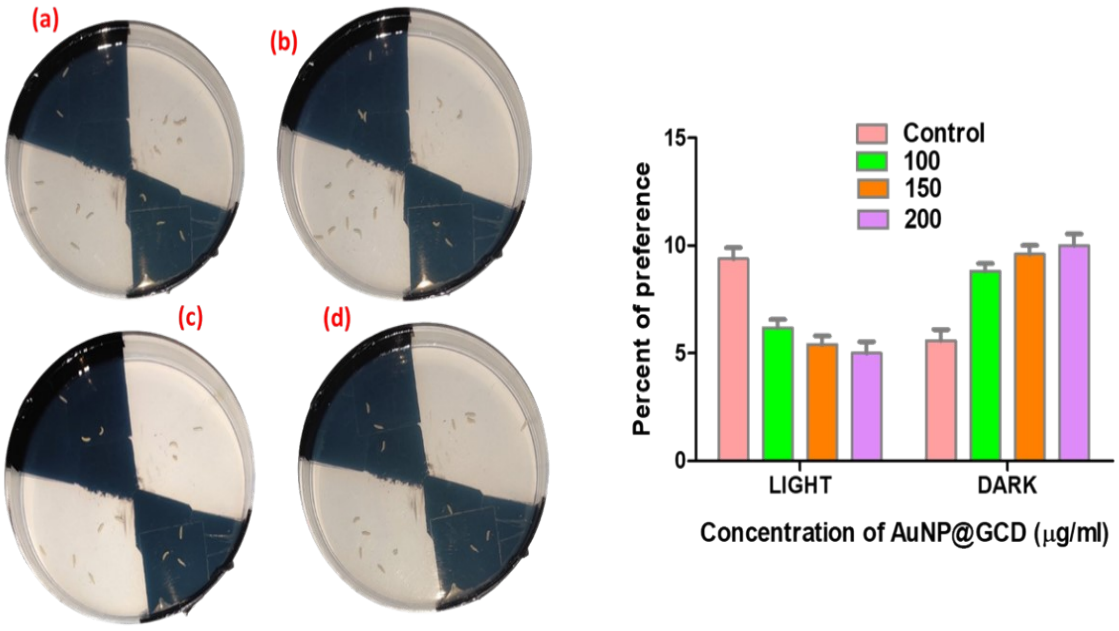


**Figure 22**

**Table S1** Hydrodynamic size of GCD after APBA@AuNP addition

| GCD (50µg/mL) | GCD + APBA@AuNP(µM) | Particle size(nm) |
|---|---|---|
| **50** | **0** | **29** |
| **50** | **2** | **102** |
| **50** | **3** | **127** |
| **50** | **7** | **171** |
| **50** | **9** | **229** |
| **50** | **12** | **307** |
| **50** | **16** | **356** |
| **50** | **19** | **412** |
| **50** | **25** | **437** |

**Table S2** Hydrodynamic size of AuNP@GCD after DA addition

| AuNP@GCD(µg/mL) | AuNP@GCD +DA (nM) | Particle Size(nm) |
|---|---|---|
| **2** | **5** | **437** |
| **2** | **10** | **356** |
| **2** | **70** | **265** |
| **2** | **110** | **229** |
| **2** | **150** | **198** |
| **2** | **190** | **171** |
| **2** | **270** | **139** |
| **2** | **310** | **112** |

**Table S3** Förster and donor-acceptor distance between the GCD and different Au NPs concentration**.**

| Donor/Acceptor | $R_0$(Å) | r (Å) |
|---|---|---|
| **GCD + Au (1µM)** | **46.85** | **36.24** |
| **GCD + Au (2µM)** | **46.80** | **35.36** |
| **GCD + Au (3µM)** | **44.77** | **34.23** |
| **GCD + Au (5µM)** | **44.69** | **34.12** |
| **GCD + Au (7µM)** | **43.62** | **33.47** |
| **GCD + Au (9µM)** | **43.21** | **33.19** |
| **GCD + Au (12µM)** | **43.10** | **32.95** |
| **GCD + Au (16µM)** | **42.32** | **32.12** |
| **GCD + Au (19µM)** | **42.13** | **31.89** |
| **GCD + Au (22µM)** | **42.09** | **31.10** |
| **GCD + Au (25µM)** | **41.85** | **30.56** |

**Table 4** Fluorescence study of dopamine in blood serum

| Sample no. | DA spiked(nM) | Human | Found (%) (nM) | Recovery (%) (µM) |
|---|---|---|---|---|
| 1 | 100 | | 101.23 | 101.23 |
| | 120 | Blood | 121.31 | 101.09 |
| | 140 | | 140.13 | 100.09 |
| 2 | 100 | | 101.43 | 101.43 |
| | 120 | Blood | 120.53 | 100.44 |
| | 140 | | 140.51 | 100.36 |
| 3 | 100 | | 100.53 | 100.53 |
| | 120 | Blood | 120.67 | 100.55 |
| | 140 | | 140.29 | 100.20 |

| **Table 5** Freeze thaw condition (-70$^0$c to room temperature) | | | | |
|---|---|---|---|---|
| | **Cycle-1(nM)** | **Cycle-2(nM)** | **Cycle-3(nM)** | **Cycle-4(nM)** |
| **Serum-1** | **10.45** | **10.31** | **10.63** | **10.81** |
| **Serum-2** | **30.37** | **30.79** | **30.64** | **30.43** |
| **Serum-3** | **70.54** | **70.13** | **70.57** | **70.41** |

**Table 6** A comparison of the sensor performance with similar work

| **Material** | **Detection method** | **LOD** | **LDR** | **Reference** |
|---|---|---|---|---|

| | | | | |
|---|---|---|---|---|
| **Y-CQDs** | **Fluorescence** | **0.03 µM** | **0.05 – 150 µM** | **16** |
| **N, S-CQDs** | **Fluorescence** | **7.15nM** | **2.23 -44.3 µM** | **17** |
| **N-CQDs** | **Electrochemical** | **4.7 µM** | **0- 2 mM** | **18** |
| **CD and N-CD** | **Fluorescence** | **5.54 & 5.12 µM** | **3.3 µM – 0.5 mM & 3.3 µM -0.4 mM** | **19** |
| **CDots-AuNCs** | **Fluorescence** | **2.9 nM** | **5 - 180 nM** | **20** |
| **AFC-CDs** | **FL and Colorimetry** | **0.29 & 2.31 µM** | **0.3-7 & 3-100 µM** | **21** |
| **CuNC@N-GQD** | **Electrochemical** | **0.000001 µM** | **0.000001-1 µM** | **22** |
| **Au-GQDs-Nafion/GCE** | **Electrochemical** | **0.84µM** | **2-50 µM** | **23** |
| **AuNP@GCD** | **Fluorescence & Electrochemical** | **0.0025 µM& 0.00026 µM** | **30nM -310nM & 0.09M -1 pM** | **This Work** |

**Table 7** Electrochemical sensing study of DA in real human serum

| Sample | Spiked (nM) | Serum | Found(%) | Recovery(%) |
|---|---|---|---|---|
| 1 | 5 | Blood | 5.034 | 100.68 |
| 2 | 10 | Blood | 10.174 | 101.74 |
| 3 | 15 | Blood | 15.234 | 101.56 |

The equation to calculate fluorescence lifetime is: $I(t) = I_o * \exp(-t/\tau)$ ----------(1)

LOD calculation for fluorescence sensing: LOD = 3S/M ----------(2)

Where SD refers to standard deviation and ṕ slope of linear regression curve

LOD Calculation in electrochemical sensing: LOD = 3S/M ----------(3)

S – The standard deviation of the current responses of blank

M -Slope of the linear plot

**Reference**


**1.** Pattnayak, B. C., & Mohapatra, S. *Spect. Acta Part A: Mole. and Biomol. Spectro*. **2023**, *286*, 122009.

**2.** Saisree, S., JS, A. N., & Sandhya, K. Y. *J. Mater. Chem. B*. **2022**, *10*, 3974-3988.

**3**. Behera, L., Mishra, L., Mishra, M., & Mohapatra, S. *J. Mater. Chem. B*. **2024**, *12*, 5181-5193.

**4.** Pappus, S. A., Mishra, M. *Cellular and molecular toxicology of nanoparticles*. **2018**,1048,311-322

**5.** Bag, J.; Mukherjee, S.; Ghosh, S. K.; Das, A.; Mukherjee, A.; Sahoo, J. K.; Tung, K. S.; Sahoo, H.; Mishra, M. *Int. J. Biol. Macromol*. **2020**, 165, 333−345

**6.** Nayak, N.; Mishra, M., *Springer Protocols Handbooks*, *Springer*. **2020**, 123−134

**7.** Mishra, P.K.*; Biomolecules*. **2019**, 9, 363

**8.** Shen, J.*; Chemosphere*. **2021**, 283, 131289

**9**. Spierer, A.N., *J. Exp. Biology*. **2021**,224,229377

**10**. Priyadarsini, S.; *Environ. Sci. Pollut. Research*. **2019**, 26,19560-19574

**11**. Grillner, S; A. El Manira*. Physiological reviews*, **2019**

**12**. Mishra, M. *Springer* **2020**

**13**. Sabat, D., *Physiology Behavior*. **2016**. 167, 76-85

**14**. Bag, J.; Mukherjee, S.; Tripathy, M.; Mohanty, R.; Shendha, P. K.; Hota, G.; Mishra, M. *J. Clust. Sci.* **2022**, 1, 1572

**15**. Kumar, A. S.; Sundararajan, V.; G Venkatasubbu, D.; Sheik Mohideen, S. *Mater. Today Proc*. **2022**, 65, 207−214

**16.** Cao, X., Shao, C., Zhang, C., Liang, M., Wang, Y., Cheng, J., & Lu, S. *Anal. Methods*. **2022**, *14*, 1342-1350.

**17**. Mondal, S., Sarkar, O., Raut, J., Mandal, S. M., Chattopadhyay, A., Sahoo, P. *ACS Appl. Bio Materials*. **2024**,*7*, 4690-4701.

**18.** Paulo-Mirasol, S., Izquierdo, C., Alemán, C., Armelin, E., & Torras, J. *Appl. Surface Science*. **2023**, *626*, 157241.

**19.** Tiwari, A., Walia, S., Sharma, S., Chauhan, S., Kumar, M., Gadly, T., Randhawa, J. K. *J. Mate. Chem. B*. **2023**, *11*, 1029-1043.

**20.** He, Y. S., Pan, C. G., Cao, H. X., Yue, M. Z., Wang, L., & Liang, G. X. *Sens. Actuator Chem. B* **2018**,*265*, 371-377.

**21.** Sun, P., Shang, M., Xie, R., Gao, Y., Tian, M., Dai, Q., & Chai, F. *Food Chemistry*. **2024**, *445*, 138794.

**22**. Saisree, S., JS, A. N., & Sandhya, K. Y. *J. Mater. Chemistry B*. **2022**, *10*, 3974-3988.

**23**. Jang, H. S., Kim, D., Lee, C., Yan, B., Qin, X., & Piao, Y. *Inorg. Chem. Commun*. **2019**, *105*, 174-181.